

Biased Gene Conversion Constrains Adaptation in *Arabidopsis thaliana*

Tuomas Hämälä¹ and Peter Tiffin

Department of Plant and Microbial Biology, University of Minnesota, St. Paul, Minnesota 55108

ORCID IDs: 0000-0001-8306-3397 (T.H.); 0000-0003-1975-610X (P.T.)

ABSTRACT Reduction of fitness due to deleterious mutations imposes a limit to adaptive evolution. By characterizing features that influence this genetic load we may better understand constraints on responses to both natural and human-mediated selection. Here, using whole-genome, transcriptome, and methylome data from >600 *Arabidopsis thaliana* individuals, we set out to identify important features influencing selective constraint. Our analyses reveal that multiple factors underlie the accumulation of maladaptive mutations, including gene expression level, gene network connectivity, and gene-body methylation. We then focus on a feature with major effect, nucleotide composition. The ancestral vs. derived status of segregating alleles suggests that GC-biased gene conversion, a recombination-associated process that increases the frequency of G and C nucleotides regardless of their fitness effects, shapes sequence patterns in *A. thaliana*. Through estimation of mutational effects, we present evidence that biased gene conversion hinders the purging of deleterious mutations and contributes to a genome-wide signal of decreased efficacy of selection. By comparing these results to two outcrossing relatives, *Arabidopsis lyrata* and *Capsella grandiflora*, we find that protein evolution in *A. thaliana* is as strongly affected by biased gene conversion as in the outcrossing species. Last, we perform simulations to show that natural levels of outcrossing in *A. thaliana* are sufficient to facilitate biased gene conversion despite increased homozygosity due to selfing. Together, our results show that even predominantly selfing taxa are susceptible to biased gene conversion, suggesting that it may constitute an important constraint to adaptation among plant species.

KEYWORDS deleterious mutations; biased gene conversion; machine-learning; DFE-alpha; evolutionary simulations; *Arabidopsis*

THE reduction of fitness due to recurrent deleterious mutations can constrain adaptive evolution (Haldane 1937; Muller 1950; Crow 1970; Charlesworth and Charlesworth 1998; Agrawal and Whitlock 2012). The extent of this genetic load depends on the efficacy of purifying selection, which may differ between species and populations due to factors such as mating-system and demographic history (Muller 1964; Ohta 1973; Lynch and Gabriel 1990; Charlesworth *et al.* 1993; Nordborg 2000). However, the strength of purifying selection also varies within individual genomes, so that some chromosomal regions are more prone to accumulate deleterious variants than others (Hill and Robertson 1966; Felsenstein 1974; Chun and Fay 2011; Hartfield and Otto

2011). Identifying features that influence this variation not only informs about the limits of adaptation but also may provide insight into processes such as the evolution of sexual reproduction (Charlesworth *et al.* 1993; Peck 1994; Charlesworth and Charlesworth 1998; Keightley and Otto 2006).

Features influencing genetic load within a genome are not well resolved, although some common patterns have been established. For instance, in nearly all studied taxa, the expression level of a gene is positively associated with the strength of purifying selection, suggesting that highly expressed genes tend to have essential roles in physiology and development (Koonin 2011). The same likely holds true for genes occupying central positions within gene networks, as multiple studies have found evidence that highly connected genes are under strong selective constraint (Rausher *et al.* 1999; Fraser *et al.* 2002; Papakostas *et al.* 2014; Josephs *et al.* 2017). Both theoretical (Muller 1964; Hill and Robertson 1966; Felsenstein 1974; Hartfield and Otto 2011) and empirical (Chun and Fay 2011; Zhang *et al.*

Copyright © 2020 by the Genetics Society of America

doi: <https://doi.org/10.1534/genetics.120.303335>

Manuscript received March 22, 2020; accepted for publication May 14, 2020; published Early Online May 15, 2020.

Supplemental material available at figshare: <https://doi.org/10.25386/genetics.12284174>.

¹Corresponding author: Department of Plant and Microbial Biology, University of Minnesota, 1479 Gortner Ave., St. Paul, MN 55108. E-mail: thamala@umn.edu

2016) studies also have established that recombination rate can modulate the strength of purifying selection, so that deleterious alleles are more efficiently removed in regions of high recombination. Moreover, features such as gene-body methylation and chromatin remodeling may be associated with genetic load, as methylated cytosines are known to have elevated mutation rate (Bird 1980; Weng *et al.* 2019), and accessible chromatin regions, indicative of *cis*-regulatory elements (Klemm *et al.* 2019), show high sequence conservation between species (Rodgers-Melnick *et al.* 2016; Lu *et al.* 2019).

GC-biased gene conversion (gBGC) also is expected to influence genetic load (Bengtsson 1990). gBGC takes place during meiotic recombination, when GC/AT heterozygotes occurring within a heteroduplex DNA are preferentially fixed to GC (as opposed to AT) nucleotides (Marais 2003; Galtier and Duret 2007; Mugal *et al.* 2015). gBGC increases the frequency of GC alleles regardless of their fitness effects, which can lead to an accumulation of deleterious mutations (Bengtsson 1990; Glémin 2010). Indeed, evidence for increased genetic load due to gBGC has been found in the human genome (Necșulea *et al.* 2011; Lachance and Tishkoff 2014). The increased frequency of GC alleles, as well as the decreased frequency of AT alleles, may also give the appearance of selection, leading to a biased view of the selection landscape (Galtier and Duret 2007; Galtier *et al.* 2009; Ratnakumar *et al.* 2010; Corcoran *et al.* 2017; Bolívar *et al.* 2018; Rousselle *et al.* 2019). The widespread occurrence of gBGC is well-established in animals (Galtier *et al.* 2001, 2009, 2018; Duret and Galtier 2009; Wallberg *et al.* 2015; Glémin *et al.* 2015; Mugal *et al.* 2015; Smeds *et al.* 2016; Corcoran *et al.* 2017; Bolívar *et al.* 2018; Rousselle *et al.* 2019) and yeast (Mancera *et al.* 2008; Lesecque *et al.* 2013), but less is known about it in plants (Glémin *et al.* 2014; Clément *et al.* 2017). The extent of gBGC is thought to be directly related to the outcrossing rate, so that it is either weak or absent in highly homozygous selfing species (Marais *et al.* 2004; Glémin 2010). Empirical data support this notion, as selfing species of the genus *Oryza* and *Collinsia* have shown weaker footprints of gBGC than outcrossing species (Muyle *et al.* 2011; Hazzouri *et al.* 2013). However, by examining the association between recombination rate and the nucleotide composition of segregating sites, Günther *et al.* (2013) found that gBGC may shape sequence variation in a predominantly selfing species, *Arabidopsis thaliana*. These results raise questions about the extent of gBGC in selfing species, and whether the accumulation of deleterious mutations and apparent signal of selection due to gBGC are limited to outcrossing taxa.

In this study, we first perform a comprehensive analysis of genomic features that likely underlie the accumulation of maladaptive mutations in *A. thaliana*. This species has recently switched from outcrossing to selfing (Bechsgaard *et al.* 2006; Tang *et al.* 2007; Bomblies *et al.* 2010; Durvasula *et al.* 2017), which has important implications for the dynamics of deleterious variants (Charlesworth

et al. 1993). Specifically, selfing reduces the effective population size (N_e), thereby weakening the efficacy of purifying selection (Bustamante *et al.* 2002). By increasing homozygosity, selfing also weakens the effects of recombination on allelic diversity (Nordborg 2000), which may run counter to the expectation that regions of high recombination accumulate few deleterious mutations (Hartfield and Otto 2011). Here, by combining whole-genome, transcriptome, and methylome data from >600 individuals, we leverage the considerable genomic and functional information available for *A. thaliana* to identify important factors associated with maladaptive mutations. We then focus on a feature with major effect—nucleotide composition. Our results suggest that gBGC has a sizable effect on sequence variation in *A. thaliana* despite selfing. We present evidence that gBGC decreases the efficacy of purifying selection by increasing the frequency of slightly deleterious mutations, which intensifies genome-wide signals of relaxed selection. Comparisons with two outcrossing species, *Arabidopsis lyrata* and *Capsella grandiflora*, suggest that gBGC leads to a footprint of relaxed purifying selection in all three species, but weakens signals of positive selection only in the two *Arabidopsis* species. Moreover, the simulations we perform demonstrate that natural levels of outcrossing are sufficient to facilitate gBGC in *A. thaliana*. Together, our results suggest that the importance of gBGC on sequence evolution is not limited to outcrossing taxa, but can have considerable genome-wide impact also in predominantly selfing species—a group that includes many of the most important crop species (Ross-Ibarra *et al.* 2007).

Materials and Methods

Data acquisition

Our main analyses are based on publicly available genome, transcriptome, and methylome data from the model-species *A. thaliana*. We focus on 645 genotypes, for which these data were collected by The 1001 Genomes Consortium (1001 Genomes Consortium 2016; Kawakatsu *et al.* 2016). These individuals represent ecotypes collected across Eurasia, North Africa, and North America.

A VCF file containing both variant and invariant sites for 1135 *A. thaliana* genotypes was downloaded from The 1001 Genomes database (<https://1001genomes.org/data/GMI-MPI/releases/v3.1/>, last accessed September 20, 2019) and filtered with VCFtools (Danecek *et al.* 2011). We retained only genotypes for which transcriptomes were sequenced by Kawakatsu *et al.* (2016). We then removed individuals identified as “relics” in the original publications, as they exhibited genetic and expression profiles that were distinct from the other individuals, leaving 645 genotypes. All indels and SNPs with more than two alleles were removed. We also removed sites with >20% missing data, and imputed the missing genotypes with Beagle 5 (Browning *et al.* 2018). Out of 120 M sites, we retained 79 M (6.3 M variable) after filtering.

Expression data for the 645 individuals were downloaded from NCBI GEO: GSE80744. According to the original publication (Kawakatsu *et al.* 2016), leaf samples were collected from plants grown in a common greenhouse environment, the RNA-seq reads aligned against the TAIR10 reference genome (Lamesch *et al.* 2012), and the per-gene read counts batch-corrected and size-normalized.

Methylation calls for the 645 individuals were downloaded from GEO: GSE43857 (Kawakatsu *et al.* 2016). For each individual, we counted the proportion of methylated cytosines (mCG, mCHG, and mCHH contexts, where H is A, T, or C) per gene. Sites with coverage <5 were removed. We estimated two features of the methylation data: the average proportion of methylated cytosines and methylation variability (measured as coefficient of variation) across the individuals.

Genomic features

We characterized multiple features that may play a role in defining the rate of sequence evolution at different regions of the *A. thaliana* genome. First, we used the TAIR10 annotation to count the number of exonic and intronic base-pairs, number of splice variants, distance to the centromere, and distance to the nearest transposable element (TE) for each gene. We then used invariant sites from the SNP-calls to calculate the percentage of guanine and cytosine bases per gene (GC%). We used ENCprime (<https://github.com/jno-vembre/ENCprime>, last accessed October 11, 2019) to estimate the effective number of codons, as reflected in the statistic N_c^e (Novembre 2002). Using data from Lu *et al.* (2019), we defined accessible chromatin regions (ACRs), indicative of *cis*-regulatory elements (Klemm *et al.* 2019). Around half of the ACRs in *A. thaliana* are found in genic regions (Lu *et al.* 2019), so we utilized two features of the data: distance to the nearest ACR and the percentage of ACR-base-pairs (ACR%) per gene.

Recombination rates (r) for genes in the *A. thaliana* genome were estimated from a crossover map covering >17,000 meiotic crossover events [based on 1920 F₂ progeny (Col-0 and Ler-0), Rowan *et al.* 2019]. The density of *de novo* mutations ($n = 2023$) from 107 mutation accumulation lines (maintained for 25 generations as single-seed descent, Weng *et al.* 2019), were used to define mutation rates (μ) for the genes. We used machine-learning-based regression modeling to predict per-gene estimates of r and μ , given their chromosomal locations. The Extremely Randomized Trees (Extra-Trees) method (Geurts *et al.* 2006), as implemented in the R package ranger (Wright and Ziegler 2017), was used for the prediction. For more information, see section *Machine-learning*.

Co-expression network

We used the R package WGCNA (Langfelder and Horvath 2008) to identify modules of co-expressed genes within the transcriptome data, as well as to estimate among-gene connectivity. A soft-thresholding power of 12 was used to calculate adjacencies for a signed co-expression network. Topological

overlap matrix (TOM) and dynamic-cut tree algorithm were used to define network modules. Modules with $\geq 90\%$ identical expression profiles were merged. Connectivity was defined as the sum of adjacencies between the focal-gene and other genes in the network.

Quantification of selective constraint

To identify putatively harmful mutations, we predicted mutational effects with SIFT4G (Vaser *et al.* 2016). SIFT predictions are based on protein conservation among homologous sequences, with rare nonsynonymous mutations assigned lower (*i.e.*, more harmful) scores. Based on analysis of known deleterious variants, this method was found to perform well in *A. thaliana* (Kono *et al.* 2018). We used the existing *A. thaliana* database (<https://sift.bii.a-star.edu.sg/sift4g/>, last accessed October 4, 2019) to annotate SNPs with MAF ≥ 0.01 among the 645 individuals, and calculated an average SIFT-score for each gene (averaged across sites at which mutational effects were predicted). High SIFT-scores indicate a low average impact of segregating mutations, reflecting strong purifying selection, whereas low SIFT-scores are due to high average impact of segregating mutations, reflecting relaxed selective constraint.

As a comparison to SIFT-scores, we estimated two statistics reflecting the efficacy of purifying selection: the ratio of nonsynonymous to synonymous nucleotide divergence (d_N/d_S) between *A. thaliana* and *A. lyrata*, and the ratio of nonsynonymous to synonymous nucleotide diversities (π_N/π_S) within *A. thaliana* (Nielsen 2005; Chen *et al.* 2017). For each gene, we also estimated pairwise nucleotide diversity across all sites, which is sensitive to factors besides purifying selection (Cutter and Payseur 2013). For d_N/d_S , orthologous gene-pairs were identified with reciprocal BLAST (Camacho *et al.* 2009) and coding sequences aligned at the codon-level with PRANK (Löytynoja and Goldman 2008). d_N and d_S were then estimated with the R package SeqinR (Charif and Lobry 2007). We used the full VCF-file to estimate pairwise nucleotide diversity (Tajima 1983) across each callable site (variant and invariant).

Machine-learning

We explored what factors best predict gene-specific measures of sequence evolution using machine-learning based regression modeling. The following features were used in the models: GC%, number of exonic and intronic base pair, number of splice variants, distance to the centromere, effective number of codons, r , μ , distance to the nearest TE, distance to the nearest ACR, ACR%, methylation level, methylation variability, connectivity, expression level, expression variability, and the co-expression module assignment. The R package ranger (Wright and Ziegler 2017) was used to train Extra-Trees (Geurts *et al.* 2006) forests to estimate the relative importance of each predictor variable. To this end, settings -splitrule “extratrees” -replace = F and -sample.fraction = 1 were used in ranger. Extra-Trees is an extension of the popular ensemble learning method, Random Forest (Breiman

2001), in which a random selection of data is used to train decision trees, and the response variable predicted based on the resulting forest. In contrast to Random Forest, which trains trees on a subset of the learning sample and defines optimal cut-points for each node, Extra-Trees are trained on the whole sample and the cut-points are chosen randomly. This approach generally reduces the risk of overfitting, potentially leading to more accurate prediction (Geurts *et al.* 2006). Indeed, with our data, Extra-Trees outperformed Random Forest by consistently yielding $\sim 1.3\times$ more accurate predictions (70% used for training and 30% used for testing). A total of 500 trees were trained in each model, and the best tuning parameters (number of variables split at each node and minimum node size) were chosen based on fivefold cross-validation, conducted with the R package *caret* (Kuhn 2008). Variable importance was estimated using a corrected Gini importance measure, which is not biased by the number or frequency of categories (Nembrini *et al.* 2018). Deviations from random expectations were assessed by permuting each predictor variable across genes. However, as training a large number of machine-learning models to estimate accurate permutation *P*-values is computationally intensive, we used a smaller number of repeats ($n = 100$) to establish a null distribution for each predictor. These empirical nulls approximately follow a normal distribution (Billingsley 2008), so we used the mean and SD to define *P*-values with the R function *pnorm*.

Derived allele frequency estimation

To better understand how nucleotide composition influences selective constraint, we partitioned segregating alleles based on their ancestral vs. derived status. We utilized three species from the family Brassicaceae as outgroups: *A. lyrata* (Hu *et al.* 2011), *Capsella rubella* (Slotte *et al.* 2013), and *Arabidopsis thaliana* (Willing *et al.* 2015). The three reference genomes were aligned against the *A. thaliana* genome with MUMmer4 (Marçais *et al.* 2018) and variants in regions showing one-to-one alignments in at least two of the three comparisons were used to estimate derived allele frequencies (DAF). First, we used a method by Keightley and Jackson (2018) to infer probabilities for derived alleles based on polymorphism data and the outgroup species. Substitutions were assumed to follow a six-parameter (R6) model, which allows for variable mutation probabilities between different nucleotides (Keightley and Jackson 2018). The uncertainty in the assignment of derived alleles was then directly incorporated into the DAF estimation:

$$\text{DAF} = \frac{\sum_{i=1}^n P(A_i = \text{derived})x_{Ai} + P(a_i = \text{derived})x_{ai}}{\sum_{i=1}^n x_{Ai} + x_{ai}}$$

where x_{Ai} and x_{ai} are the counts of alleles A_i and a_i in a site i , and n is the number of segregating sites in a gene. We employed the common division of nucleotides based on their number of hydrogen bonds, strong (S: G or C) and weak (W: A or T), to estimate DAF for classes: WS, SW, and SS+WW (the first letter or each pair corresponds to the ancestral allele

and the second letter corresponds to the derived allele). gBGC tends to increase the frequency of derived S alleles and decrease the frequency of derived W alleles, and therefore the relative frequencies of WS, SW, and SS+WW alleles provide insight into the strength of gBGC at different regions of the genome. As a more specific measure of gBGC, we estimated the ratio of WS to SW (WS/SW) for each gene, with estimates >1 indicating an excess of segregating S alleles, potentially caused by gBGC. We note that mutation probabilities in the R6 substitution model are symmetric (*e.g.*, $C \rightarrow T$ and $T \rightarrow C$ are represented by a single parameter) and therefore asymmetries in mutation rates, caused *e.g.*, by the hypermutability of methylated cytosines, are not directly accounted for. To examine to what extent such asymmetries might bias the derived-allele probabilities, we used a parsimony-based approach (all three outgroup-species were required to carry the same allele) to estimate mutation proportions between each of the four nucleotides. Our results indicate that $C \rightarrow T$ (0.18) and $G \rightarrow A$ (0.18) transitions have been the most common mutations, followed by the opposite $T \rightarrow C$ (0.11) and $A \rightarrow G$ (0.11) transitions. By contrast, transversion have been less common and more symmetric (Supplemental Material, Figure S1). The observed transitional asymmetry may therefore cause the derived-allele probabilities to be overestimated at SW sites, leading to an increase of SW alleles being sampled, and underestimated at WS sites, leading to a decrease of WS alleles being sampled. Given that this pattern is opposite to what is expected under gBGC, the asymmetry should, on average, make our results conservative.

DFE and α

We estimated the distribution of fitness effects (DFE) using DFE-alpha (Keightley and Eyre-Walker 2007). DFE-alpha models the DFE as a gamma distribution governed by the mean strength of selection ($N_e s$) and the shape parameter β . The DFE can range from leptokurtic (L-shaped) to platykurtic (spike-shaped), providing insight into the strength of purifying selection (Eyre-Walker and Keightley 2007). An extension of the McDonald-Kreitman test (McDonald and Kreitman 1991) was used to estimate the rate of positive selection, while taking into account the number of nearly neutral mutations derived from the DFE (Eyre-Walker and Keightley 2009). Here, the ratio of nonsynonymous to synonymous polymorphisms (p_N/p_S) within species is compared against the ratio of nonsynonymous to synonymous divergence (d_N/d_S) between species. The proportion of adaptive substitutions is then estimated as: $\alpha = 1 - (p_N/p_S)/(d_N/d_S)$, and the rate of adaptive substitutions relative to the neutral mutation rate as: $\omega_A = \alpha(d_N/d_S)$.

We used the whole-genome alignments to count the number of 0-fold and fourfold substitutions in *A. thaliana*. All variant and invariant sites from the aligned regions were then used to estimate unfolded nonsynonymous and synonymous site frequency spectra (SFS), which were subsequently folded by DFE-alpha. The *A. thaliana* accessions used here are fully

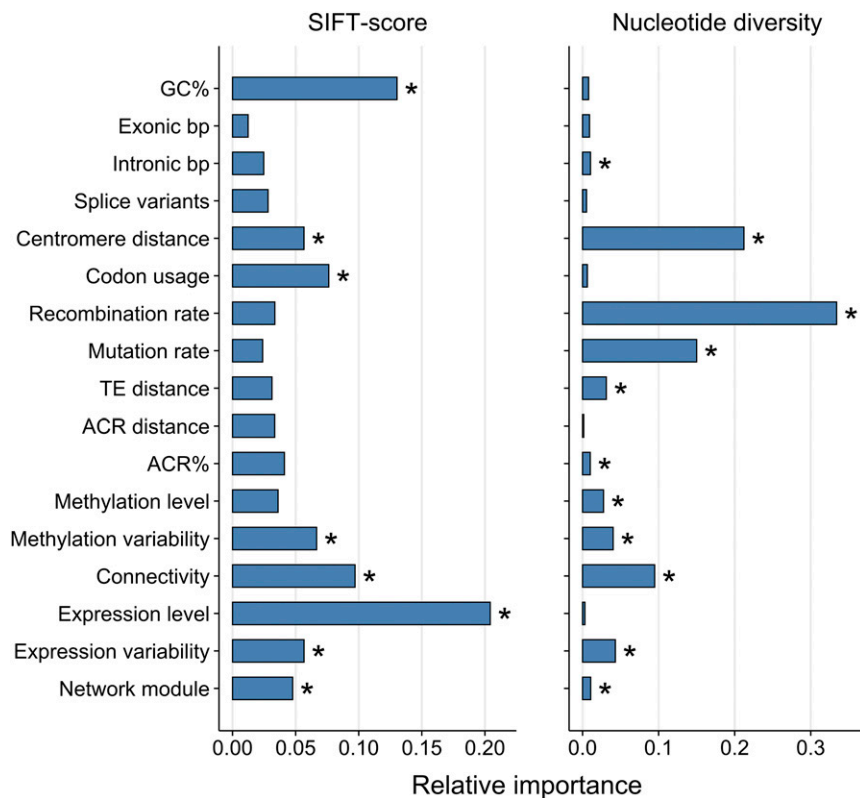


Figure 1 Variable importance from Extra-Trees models for SIFT-scores and nucleotide diversity. * $P < 0.05$ (Bonferroni corrected).

homozygous, so we treated them as haploid when estimating the SFS. To account for the uncertainty in the assignment of ancestral vs. derived alleles, which is important for the WS and SW sites, we sampled derived alleles based on their individual probabilities using the same approach as with DAF. To account for nonequilibrium population histories, two-step N_e change was included into the DFE models. Confidence intervals for DFE, α , and ω_A were estimated by fitting the models to 500 parametric bootstrap SFS. We assumed that counts in the bootstrap replicates were distributed multinomially, with number of trials corresponding to total number of sites in the SFS and the probability of success corresponding to proportion of sites in a given derived allele group. The bootstrap SFS were generated with the R function `rmultinom`.

Arabidopsis lyrata* and *Capsella grandiflora

To better assess how selfing affects gBGC, we repeated part of our analyses using whole-genome data from two outcrossing Brassicaceae species, *A. lyrata* ssp. *petraea* and *Capsella grandiflora*. For *A. lyrata*, we used 21 individuals from Jotunheimen, Norway, published as part of two studies: Mattila *et al.* (2017) and Hämälä *et al.* (2018). For *C. grandiflora*, we used 21 individuals from Zagori, Greece, published by Steige *et al.* (2017). With the *C. grandiflora* data, we followed the approach of Steige *et al.* (2017) and aligned reads against the genome of a recently (<200 KYA, Koenig *et al.* 2019) diverged species *C. rubella*, which is more contiguous than

the currently available *C. grandiflora* genome. For estimation of recombination rates, we used linkage maps constructed for both species. The *A. lyrata* map consists of 1515 markers, genotypes for 354 F_2 progeny (Hämälä *et al.* 2017), and the *C. grandiflora* map consists of 890 markers, genotyped for 550 F_2 progeny (Slotte *et al.* 2012).

For both *A. lyrata* and *C. grandiflora*, low quality reads and sequencing adapters were first removed with Trimmomatic (Bolger *et al.* 2014) and the surviving reads aligned against their respective reference genomes (*A. lyrata* v1.0, Hu *et al.* 2011; *C. rubella* v1.0, Slotte *et al.* 2013) with BWA-MEM (Li 2013). SAMtools (Li *et al.* 2009) was used to sort the alignments and remove duplicated reads. Calling of variant and invariant sites was done with BCFtools (Li 2011), using only reads with mapping quality ≥ 30 and base quality ≥ 20 . The resulting VCF-files were filtered with the following requirements: site quality ≥ 20 , genotype quality ≥ 20 , read coverage ≥ 6 , and missing data in <20% of individuals. All indels and SNPs with more than two alleles were further removed. For *A. lyrata*, we retained 110 M (4.9 M variable) out of 150 M sites, and, for *C. grandiflora*, we retained 100 M (7.3 M variable) out of 120 M sites. These data were used to estimate GC%, π_N/π_S , DFE, α , and ω_A using the same methods as for *A. thaliana*.

Forward simulations

The *A. thaliana* data are derived from accessions that were selfed multiple times between collection and sequencing, so

Table 1 Spearman's rank correlation between genomic features and two measures of sequence evolution

Feature	SIFT-score		Nucleotide diversity	
	Pairwise	Partial ^a	Pairwise	Partial ^a
GC%	0.17*	0.10*	-0.05*	-0.03*
Exonic bp	0.01	~0	~0	-0.03*
Intronic bp	-0.01	~0	-0.08*	-0.01
Splice variants	-0.05*	-0.04*	-0.01	~0
Centromere distance	-0.06*	-0.05*	-0.27*	-0.11*
Codon usage	-0.08*	-0.03*	~0	0.03*
Recombination rate	0.05*	0.02*	0.29*	0.13*
Mutation rate	0.01	~0	0.10*	0.04*
TE distance	-0.02*	~0	-0.14*	-0.02
ACR distance ^b	-0.09*	0.01	-0.10*	~0
ACR% ^b	0.11*	0.01	0.11*	0.04*
Methylation level	-0.02	~0	-0.05*	0.06*
Methylation variability	0.01	0.01	0.12*	0.08*
Connectivity	0.12*	0.02	-0.17*	-0.12*
Expression level	0.25*	0.16*	-0.06*	-0.06*
Expression variability	-0.10	-0.04*	0.18*	0.09*

^a Partial correlation after controlling for all other features (Kim 2015).

^b Accessible chromatin region.

* $P < 0.05$ (Bonferroni corrected).

they cannot be used to estimate the expected number of heterozygous sites that are susceptible to gBGC. We therefore conducted forward simulations with SLiM 3 (Haller and Messer 2019) to estimate to what extent gBGC could be expected in natural populations. Selfing in *A. thaliana* has evolved relatively recently, likely between 500 K and 1 M generations ago (Bechsgaard *et al.* 2006; Tang *et al.* 2007; Durvasula *et al.* 2017). For this reason, we started by establishing a single fully outcrossing population of $N = 50,000$ individuals, approximately corresponding to twice the current N_e estimate of European *A. thaliana* (Durvasula *et al.* 2017). After a burn-in of $10N$ generations, the population switched to (predominant) selfing, at which time N was reduced to 25,000 (as expected under selfing; Pollak 1987). We considered four rates of outcrossing: 0, 5, 10, and 15%, approximately corresponding to outcrossing rates estimated for natural *A. thaliana* populations from Germany (Bombliès *et al.* 2010; Sellinger *et al.* 2020). Mutation rate (μ) was set to 6.95×10^{-9} (Weng *et al.* 2019), with nucleotide replacements following a Jukes-Cantor model (Jukes and Cantor 1969) without any GC/AT bias. We considered three crossover rates (r) based on our gene-specific estimates: weak 2.3×10^{-8} (minimum estimate), moderate 4.0×10^{-8} (average estimate), and high 7.3×10^{-8} (maximum estimate). The N , μ , and r parameters were rescaled by a factor 10 to reduce computation time, while retaining the same product of $N\mu$ and Nr as the unscaled data (Kim and Wiehe 2008). Based on Yang *et al.* (2012), gene conversions were assumed to outnumber crossovers by a factor of 50 and to have an average track length of 553 bp. For parameter governing the GC over AT repair bias, we considered three values: 5, 10, and 20%, approximately corresponding to different levels of bias estimated for *A. thaliana* (Yang *et al.*

2012; Wijnker *et al.* 2013; Liu *et al.* 2018). In total, we simulated 100×50 kb regions with each parameter combination. Following the switch to selfing, simulations were run 100 K generations (1 M/10, the rescaling parameter), during which the extent of gBGC was defined by estimating WS/SW and GC% as with the observed data. We note that the efficacy of gBGC can be dependent on the effective population size (Duret and Galtier 2009), so the rescaling of N , μ , and r might diminish the effects of gBGC. However, by conducting a subset of the simulations with unscaled parameters, we found that although rescaling has a slight effect on the absolute values of WS/SW and GC%, it does not influence the relative patterns arising from selfing (Figure S2). Therefore, conclusions drawn from these results should not be greatly affected by the parameter-scaling.

Data availability

The authors state that all data necessary for confirming the conclusions presented in the article are represented fully within the article. Supplemental figures and tables, a compiled table of genomic features, and a code for running the simulations are available at figshare: <https://doi.org/10.25386/genetics.12284174>.

Results

Genomic features influence selective constraint

We used machine-learning based modeling to examine how genomic features influence the accumulation of deleterious mutations at different regions of the *A. thaliana* genome. To this end, we estimated average SIFT-scores for 24,855 protein-coding genes, of which 18,070 had complete data for the 16 features used as predictors in our Extra-Trees models (Figure S3). The two other statistics reflecting the strength of purifying selection, d_N/d_S and π_N/π_S , produced similar results as SIFT (Figure S4 and Table S1), so here we focus on identifying factors affecting SIFT-scores. Multiple features had an influence on SIFT-scores (Figure 1), with expression level and GC% having largest effects. Both features were positively correlated with SIFT-scores (Table 1), indicating that mutations segregating at >0.01 frequency in highly expressed genes and GC-rich genes were less deleterious than the genome-wide average. Genes with greater connectivity in a co-expression network also had higher than average SIFT-scores, whereas increase in the effective number of codons (*i.e.*, lower codon-usage bias, Novembre 2002), variability in gene-body methylation, and distance from the centromere had the opposite effects (Figure 1 and Table 1). An additional important factor was the module assignment from a co-expression network (30 modules in total), indicating that genes from each module have more similar SIFT-scores than expected by chance. This similarity suggests that genes within the modules respond to correlated selection pressures, possibly due to shared biological function (Hämälä *et al.* 2020). Interestingly, effect of recombination rate on average

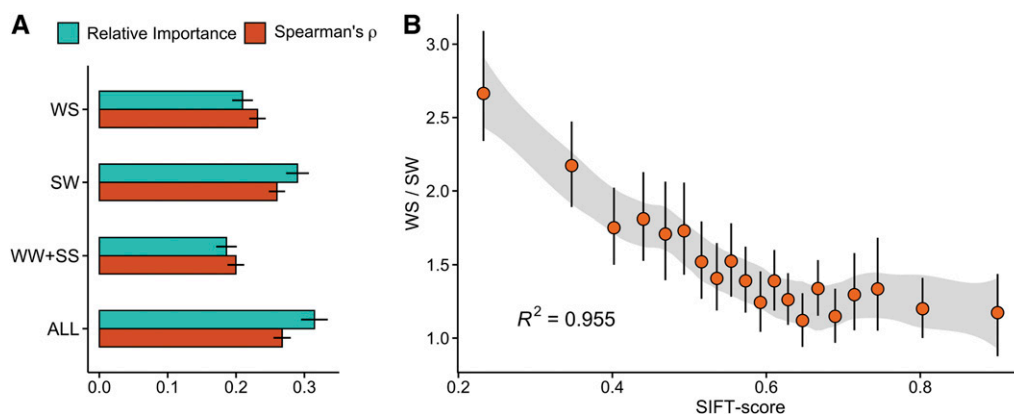


Figure 2 The effect of gBGC on selective constraint. (A) Importance from an Extra-Trees model with SIFT-scores as the response and the four DAF classes as predictors, and Spearman's rank-correlation ρ between SIFT-scores and DAF classes. Error bars show 95% CIs. (B) Relationship between WS/SW, a measure of gBGC, and SIFT-scores. Data were split into 20 bins of equal size based on their SIFT-scores. Figure shows means (circles) and 95% CIs (error bars) estimated for each bin. Also shown are 95% CI and R^2 for a loess-model (shaded area) fit on the binned data.

SIFT-scores was minor and did not exceed values from random permutations. This pattern is in stark contrast to nucleotide diversity, for which recombination rate and the distance from the centromere (arguably, a proxy for recombination rate) were clearly the best predictors, while expression level and GC% were of minor importance (Figure 1 and Table 1).

GC-content is a major predictor of selective constraint

The positive association between expression level and the strength of purifying selection (Table 1) is well-established in multiple taxa (Koonin 2011). By contrast, the relationship between nucleotide composition and selection is less explored, particularly in plants (Glémin *et al.* 2014). We therefore conducted analyses to identify factors that might explain the relationship between GC% and the accumulation of deleterious mutations. In mammals, GC% is positively correlated with recombination rate, which is thought to arise from gBGC increasing the fixation probability of GC alleles in regions of high recombination (Duret and Galtier 2009). gBGC also can drive the spread of deleterious AT \rightarrow GC alleles and inhibit the spread of deleterious GC \rightarrow AT alleles. If gBGC is acting in *A. thaliana*, we would expect a positive correlation between GC% and recombination rate. However, like previous studies in *A. thaliana* (Giraut *et al.* 2011; Wijnker *et al.* 2013), we found this correlation to be negative (Spearman's $\rho = -0.12$, $P < 2 \times 10^{-16}$). The Extra-Trees model also revealed that recombination rate is of minor importance in explaining variation in GC% (Table S2), being far less important than methylation variability, methylation level, expression level, codon usage, and intron length.

The minor importance of recombination rate in explaining GC% suggests that gBGC may not have an important effect on nucleotide composition in *A. thaliana*. However, it also is possible that GC% is a poor proxy for gBGC in predominantly selfing species. For this reason, we estimated DAF for each of three groups: WS (ancestral allele A or T, derived allele G or C; AT \rightarrow GC), SW (ancestral allele G or C, derived allele A or T; GC \rightarrow AT), and WW+SS (ancestral and derived A or T,

and ancestral and derived G or C; AT \rightarrow AT and GC \rightarrow GC). If gBGC is affecting nucleotide composition in *A. thaliana*, we would expect gBGC to contribute to the spread of WS alleles, inhibit the spread of SW alleles, and not affect the evolution of WW+SS alleles. Consistent with this notion, we found that average DAF was highest for WS alleles (DAF = 0.10), lowest for SW alleles (DAF = 0.08), and intermediate for WW+SS alleles (DAF = 0.09; $P < 2 \times 10^{-16}$, Wilcoxon rank-sum test). Moreover, by estimating synonymous Tajima's D (Tajima 1989) for sites with derived-allele probability >0.8 , we found that, compared to the unbiased WW+SS sites ($D = -0.95$, 95% CI: -0.96 to -0.94), the SFS was shifted toward common variants at WS sites ($D = -0.84$, 95% CI: -0.85 to -0.83) and shifted toward rare variants at SW sites ($D = -1.00$, 95% CI: -1.01 to -0.99); a pattern indicative of gBGC (Lachance and Tishkoff 2014). The frequency of segregating alleles thus suggests that gBGC may shape nucleotide variation in *A. thaliana* despite it only having a minor role in the genome-wide GC%, which is more strongly affected by factors such as gene-body methylation, expression level, and gene structure (Table S2).

gBGC affects the efficacy of purifying selection

To assess whether gBGC can lead to an accumulation of deleterious mutations in *A. thaliana*, we examined the relationship between DAF and SIFT-scores. Overall, there was a positive correlation between the two measures (Figure 2A), indicating that high frequency derived alleles have, on average, lower negative impact on fitness. However, by comparing the DAF at each of the three allelic classes, we saw that the frequency of SW alleles was a better predictor of SIFT-scores than the frequency of either WS or WW+SS alleles (Figure 2A). The correlation between SW-allele frequency and SIFT-scores also was more highly positive than in the other DAF classes, indicating that genes with predominantly strong ancestral alleles tend to have segregating mutations that are less harmful. gBGC could reduce the impact of

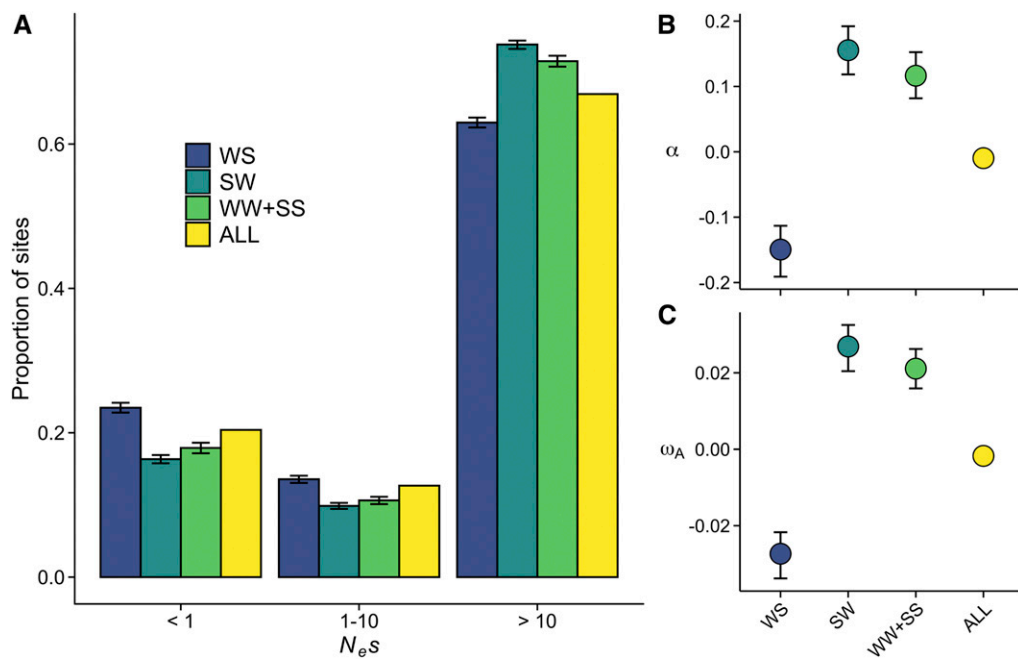


Figure 3 Apparent strength of negative and positive selection in *A. thaliana* ($n = 645$). (A) The distribution of fitness effects (DFE). Nonsynonymous sites were divided into three bins based on the strength of purifying selection ($N_e s$): nearly neutral, intermediate, and highly deleterious, respectively. (B) The proportion of sites by positive selection (α). (C) The rate of adaptive substitutions relative to the neutral mutation rate (ω_A). For all three figures, error bars show 95% CIs (CIs are too narrow to show for ALL-sites).

segregating mutations at these genes by decreasing the frequency of derived alleles, most of which are deleterious (Eyre-Walker and Keightley 2007). Under this model, the opposite pattern is expected at genes with predominantly weak ancestral alleles, as gBGC can increase the frequency of slightly deleterious mutations (Bengtsson 1990; Glémin 2010).

To test this hypothesis, we examined the relationship between WS/SW and SIFT-scores. We found a clear negative trend between the two measures; genes with low average SIFT-scores (*i.e.*, more harmful mutations) had a greater excess of derived S alleles (Figure 2B; similar associations were also found for d_N/d_S and π_N/π_S , Figure S5). Although the derived allele probabilities at WS and SW sites are likely influenced by asymmetric mutation rates (Figure S1), on average this bias would increase SW alleles and decrease WS alleles, making the trend observed here conservative. We further found that mutation rate and WS/SW are not correlated (Spearman's $\rho \approx 0$), indicating that variation in WS/SW is not driven by mutation bias. On the other hand, these results might be affected by the presence of methylated cytosines, which have the highest SW mutation rates in the *A. thaliana* genome (Weng *et al.* 2019). Polarization errors at such sites are more likely, which could lead to an apparent excess of high frequency WS mutations (Glémin *et al.* 2015), and thus inflate the WS/SW at genes with more hypermutable sites. To address this potential issue, we fit the following linear model to the data: SIFT-score = WS/SW + mC%, where mC% is the average density of methylated cytosines within a gene. The model showed that mC% has little effect on the association between WS/SW and SIFT-scores (without mC% as a cofactor: $\beta_{WS/SW} = -0.087$, with mC% as a cofactor: $\beta_{WS/SW} = -0.085$; $P < 2 \times 10^{-16}$ for both),

indicating that the signal of gBGC is not biased by hypermutable sites. Our results are therefore consistent with gBGC preventing the purging of deleterious mutations at genes with predominantly weak ancestral alleles, while facilitating their removal at genes with predominantly strong ancestral alleles. In fact, including WS/SW into our Extra-Trees model revealed that it is among the best predictors of SIFT-scores, exceeded only by expression level and GC% (relative importance: expression level = 0.19, GC% = 0.12, WS/SW = 0.11). These results lead us to conclude that gBGC is strong enough in *A. thaliana* to influence the efficacy of purifying selection.

gBGC leads to a signal of relaxed selection in *A. thaliana*

A characteristic feature of gBGC is that the increased frequency of S alleles and the decreased frequency of W alleles may give the appearance of selection (Galtier and Duret 2007). We therefore examined whether gBGC in *A. thaliana* is prominent enough to alter the estimates of selection. DFE estimated for different DAF classes revealed that WS had more, and SW fewer, nonsynonymous sites in the nearly neutral category ($N_e s < 1$) than the genome-wide average, indicating relaxed purifying selection at WS sites and stronger than average selective constraint at SW sites (Figure 3A). Consistent with previous estimates for *A. thaliana* (Fay 2011; Slotte *et al.* 2011; Gossmann *et al.* 2012), the genome-wide α and ω_A were close to zero, suggesting that positive selection has little effect on shaping nucleotide diversity in *A. thaliana*. By contrast, the α and ω_A estimates for WS sites were clearly negative, and the estimates for SW sites were clearly positive (Figure 3, B and C). These results give the appearance of WS sites evolving slower than average rate and SW sites evolving faster than average rate. The DFE, α , and

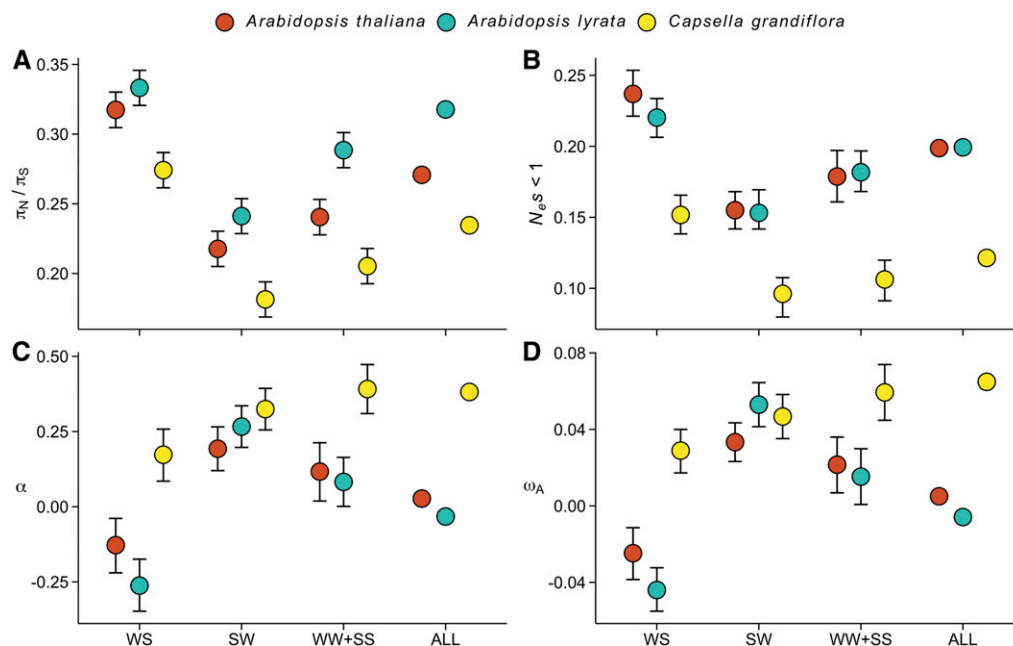


Figure 4 The effect of gBGC on measures of protein evolution in three Brassicaceae species. Analyses were conducted using the same number of chromosomes ($n = 42$) from each species. (A) The ratio of nonsynonymous to synonymous nucleotide diversities (π_N/π_S). (B) The proportion of nearly neutral mutations ($N_e s < 1$). (C) The proportion of sites fixed by positive selection (α). (D) The rate of adaptive substitutions relative to the neutral mutation rate (ω_A). For all four figures, error bars show 95% CIs.

ω_A results stay unchanged when sites that are most susceptible to gene-body methylation (mCG) were removed (Figure S6), indicating that hypermutable sites have little effect on the estimates of selection. Moreover, by conducting this analysis separately for four largest admixture groups defined by The 1001 Genomes Consortium (2016), we confirmed that our results are not biased by population structure, as each group showed patterns similar to those of the complete dataset (Figure S7).

The α and ω_A are based on the ratios of nonsynonymous to synonymous divergence (d_N/d_S) and nonsynonymous to synonymous polymorphisms (p_N/p_S). In general, positive estimates are the result of d_N/d_S exceeding p_N/p_S , whereas the reverse is true for negative estimates. The contrasting estimates at WS and SW sites can therefore arise if gBGC has different effects on divergence and polymorphism rates at these sites. We found that, compared to the unbiased WW+SS sites, both d_N/d_S and p_N/p_S (excluding polymorphisms with frequency $< 15\%$; Charlesworth and Eyre-Walker 2008) were increased at WS sites and decreased at SW sites (Figure S8). However, the difference between the p_N/p_S estimates (WS = 0.22, SW = 0.14) was greater than between the d_N/d_S estimates (WS = 0.21, SW = 0.17), consistent with the notion that gBGC can prevent the removal of slightly deleterious polymorphisms at WS sites, while facilitating their removal at SW sites. Overall, our results suggest that gBGC contributes to the signal of decreased selection-efficacy in *A. thaliana* (genome-wide α and $\omega_A \approx 0$). More accurate estimates of selection may be obtained by examining WW+SS sites, which should not be affected by gBGC. Estimates of α and ω_A at WW+SS sites were clearly greater than zero ($\alpha = 0.12$, 95% CI: 0.09 to 0.14; $\omega_A = 0.022$, 95% CI: 0.017 to 0.025), suggesting that positive

selection has been more important in shaping nucleotide diversity in *A. thaliana* than previously thought.

Evidence of gBGC in outcrossing relatives *A. lyrata* and *C. grandiflora*

To examine the role of selfing in gBGC, we estimated π_N/π_S , DFE, α , and ω_A for two related outcrossing species, *A. lyrata* and *C. grandiflora*. We used population data originating from Norway (*A. lyrata*, $n = 21$) and Greece (*C. grandiflora*, $n = 21$) for the two species. All else being equal, the increased heterozygosity due to outcrossing should result in stronger footprints of gBGC in *A. lyrata* and *C. grandiflora* than in *A. thaliana*. We note, however, that the two outcrossing species have very different demographic histories, with population size decline in *A. lyrata* (current $N_e < 10$ K, Hämälä *et al.* 2018; Hämälä and Savolainen 2019; Mattila *et al.* 2019) and population size increase in *C. grandiflora* (current $N_e > 500$ K, Douglas *et al.* 2015; Mattila *et al.* 2019). To test for an effect of the mating-system, we compared results from *A. lyrata* and *C. grandiflora* to a set of 42 *A. thaliana* individuals from Germany, yielding the same number of sampled chromosomes (due to full homozygosity) as the outcrossing species (note that estimates in Figure 3 are based on all 645 individuals).

Unlike in *A. thaliana*, we found a positive correlation between GC% and recombination rate in both *A. lyrata* (Spearman's $\rho = 0.09$, $P < 2 \times 10^{-16}$) and *C. grandiflora* (Spearman's $\rho = 0.07$, $P = 2 \times 10^{-16}$), suggesting that gBGC may more strongly increase the fixation probability of GC alleles in these species. Patterns of π_N/π_S (Figure 4A) and DFE (Figure 4B) were similar in the two outcrossing species and *A. thaliana*, with a signal of relaxed purifying selection at WS sites and a signal of stronger than average selective

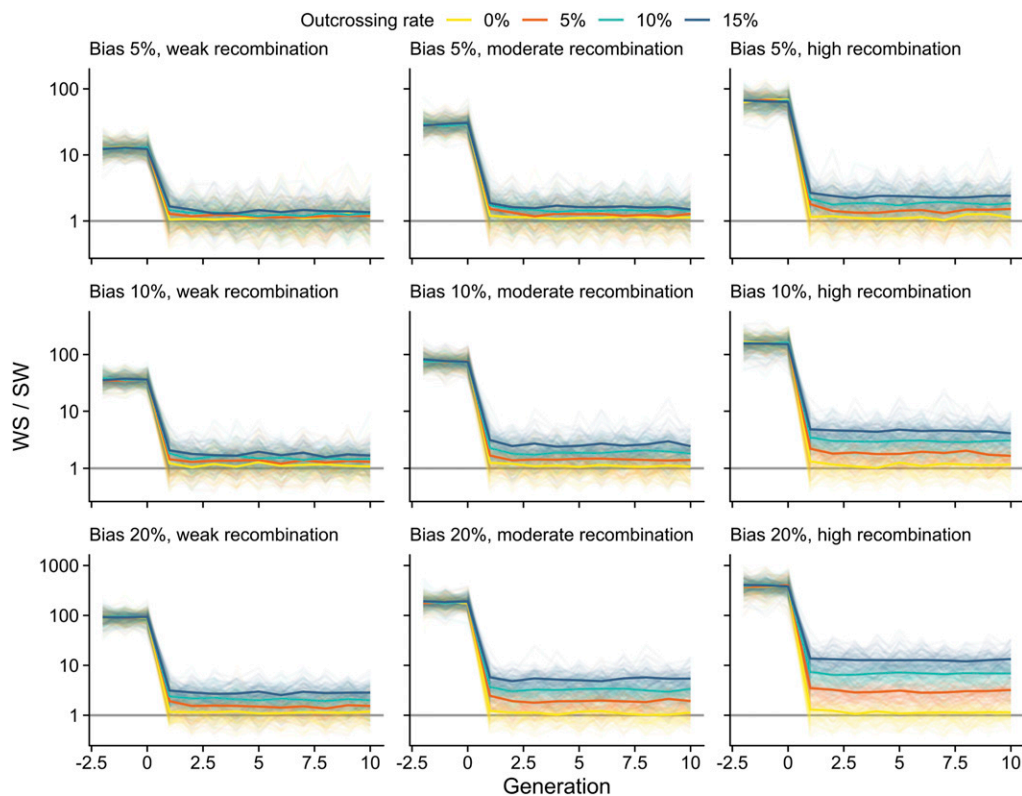


Figure 5 The simulated extent of WS/SW under gBGC. Time in number of generations is shown in the horizontal axes ($\times 10^4$ scaled, $\times 10^5$ unscaled). At time zero, population switches from full outcrossing to predominant selfing. WS/SW estimates are shown for three levels of GC over AT repair bias, three recombination rates, and four outcrossing rates. Solid colors show average estimates. Results from each of 100 simulations are shown in transparent colors. Gray horizontal lines mark the expected estimates in the absence of gBGC.

constraint at SW sites. The genome-wide estimates of α (Figure 4C) and ω_A (Figure 4D) supported previous findings by showing weak signs of positive selection in *A. lyrata* (Gossmann *et al.* 2010; Mattila *et al.* 2019) and strong signs in *C. grandiflora* (Slotte *et al.* 2010; Williamson *et al.* 2014). The estimates of α and ω_A for each of the DAF classes were similar in the two *Arabidopsis* species; compared to the genome-wide average, measures of positive selection were lower for WS sites and higher for SW sites. The unbiased WW+SS sites also had higher α and ω_A than the genome-wide average. In contrast to the *Arabidopsis* species, α and ω_A estimates showed weaker footprints (smaller deviations of WS and SW sites from the overall average) of gBGC in *C. grandiflora*. Overall, our results suggest that gBGC leads to a signal of relaxed efficacy of selection, particularly in the small- N_e species *A. thaliana* and *A. lyrata*. However, contrary to our initial expectation, the intensity of the signal was not stronger in the outcrossing species.

gBGC is expected in *A. thaliana* despite selfing

Contrary to the view that gBGC should be weak or absent in predominantly selfing species (Marais *et al.* 2004; Glémin 2010), our results suggest that it has a sizeable effect on sequence variation in *A. thaliana*. This seemingly unexpected result could arise from residual effects of recent outcrossing, and/or if natural levels of continuing outcrossing are high enough to facilitate gBGC. To evaluate this, we used forward simulations to explore the effects of a recent mating-system shift and low outcrossing rates on signals of gBGC. These

simulations revealed that both WS/SW and GC% were affected by the switch to selfing; WS/SW rapidly dropped from initial high values and the increase of GC% slowed shortly after the end of full outcrossing. As expected, stronger repair bias and higher recombination rate led to clearer footprints of gBGC (Figure 5 and Figure 6).

The composition of segregating alleles, as measured by WS/SW, was highly sensitive to the mating-system shift, and 100 K generations of selfing was enough to remove any residual effects of full outcrossing. However, despite the radical drop in WS/SW after the mating-system shift, equilibrium values were clearly affected even by low levels of ongoing outcrossing. Under complete selfing, gBGC had little influence on segregating alleles, but the effects increased rapidly with increasing outcrossing rate. At 5% outcrossing, close to an average estimated by Bomblies *et al.* (2010), WS/SW estimates deviated from the expected values under most parameter combinations, and at 15% outcrossing, close to an estimate by Sellinger *et al.* (2020), WS/SW estimates were clearly higher than in the absence of gBGC (Figure 5). The increase in GC% that was driven by gBGC during outcrossing slowed sharply, but did not decrease, following the transition to selfing. After the mating-system shift, the ongoing outcrossing had little effect on GC% during the 1 M generations examined here (Figure 6). Our simulations are therefore consistent with continuing effects of gBGC on segregating sites (WS/SW) in *A. thaliana*, whereas fixed sites (GC%) may mostly reflect patterns established during the recent outcrossing.

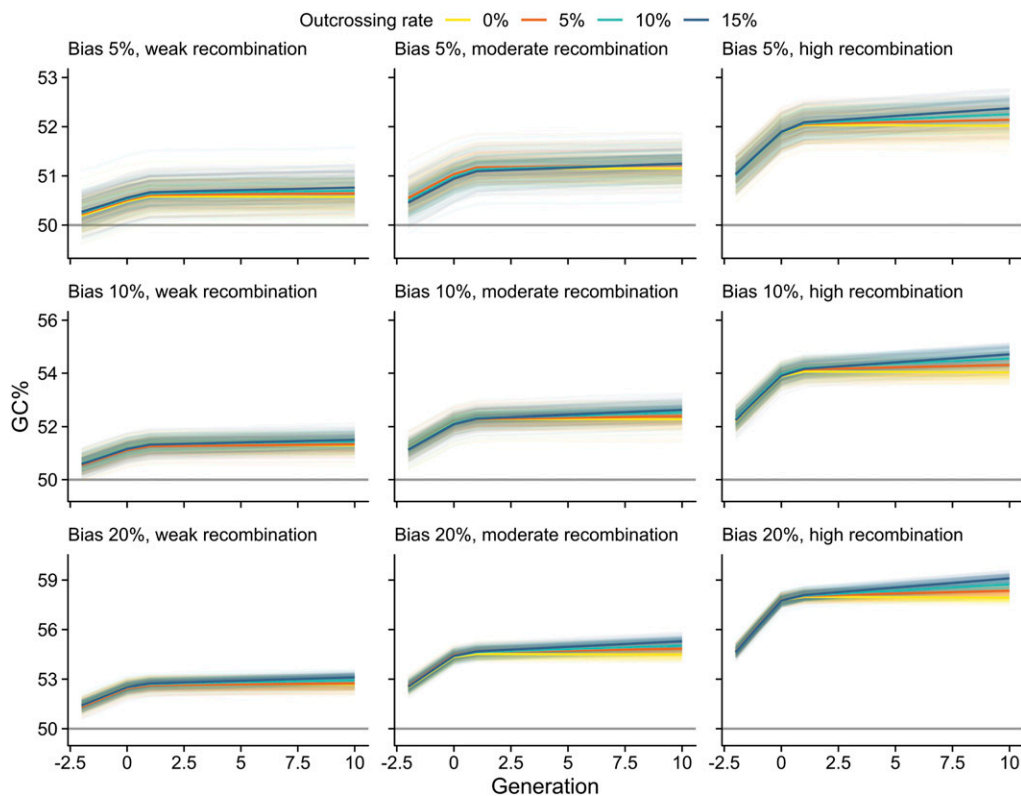


Figure 6 The simulated extent of GC% under gBGC. Time in number of generations is shown in the horizontal axes ($\times 10^4$ scaled, $\times 10^5$ unscaled). At time zero, population switches from full outcrossing to predominant selfing. GC% estimates are shown for three levels of GC over AT repair bias, three recombination rates, and four outcrossing rates. Solid colors show average estimates. Results from each of 100 simulations are shown in transparent colors. Gray horizontal lines mark the expected estimates in the absence of gBGC.

Discussion

By using whole-genome, transcriptome, and methylome data from *A. thaliana*, we have gained new insights into factors influencing selective constraint in this model-species. As expected, segregating harmful mutations are not uniformly distributed among genes, but are influenced by variation in features such as expression level, connectivity, codon usage bias, and gene-body methylation. Interestingly, we found strong evidence that GC-biased gene conversion (gBGC) shapes sequence variation in *A. thaliana*, despite the high rate of self-fertilization. As gBGC is expected to be weak or absent in selfing species (Marais *et al.* 2004; Glémin 2010), we conducted simulations to assess whether natural levels of outcrossing in *A. thaliana* can facilitate gBGC. Our results are consistent with previous findings in showing that gBGC may be undetectable under complete selfing. However, even relatively weak outcrossing of $\sim 5\%$ could result in noticeable effect, suggesting that the mating-system does not prevent gBGC from shaping nucleotide variation in predominantly selfing species such as *A. thaliana*.

A general pattern observed in mammals, birds, yeast, and grasses is that GC-content (GC%) is positively correlated with recombination rate (Eyre-Walker 1993; Duret and Galtier 2009; Pessia *et al.* 2012; Glémin *et al.* 2014; Mugal *et al.* 2015). Here, we also found such a correlation in the outcrossing species *A. lyrata* and *C. grandiflora*. This correlation is thought to arise from gBGC, as the frequency of derived GC alleles is more strongly increased in regions of high

recombination (Eyre-Walker 1993; Marais 2003). A lack of positive correlation between GC% and recombination, as in *A. thaliana*, has been interpreted as evidence against gBGC (Marais *et al.* 2004; Pessia *et al.* 2012). However, there is direct evidence for GC-biased gene conversion in *A. thaliana* (Yang *et al.* 2012), and population genetic analyses have suggested that this leads to noticeable genome-wide effects on nucleotide variation (Cao *et al.* 2011; Günther *et al.* 2013). Why then does recombination rate appear to be weakly correlated with the genomic signatures of gBGC in *A. thaliana*? Although our simulations suggest that the residual effects of outcrossing could still be seen in GC%, this association only holds if the recombination landscape has remained largely unchanged since *A. thaliana* switched to selfing. Given the variable nature of the recombination landscape (Stapley *et al.* 2017; Lloyd *et al.* 2018), this condition could be easily violated. We further found that GC% is strongly influenced by many factors, potentially confounding the signal arising from recombination and gBGC. Our results therefore suggest that the correlation between GC% and recombination rate is not an appropriate proxy for gBGC in all organisms.

Theory predicts that gBGC increases genetic load by driving the frequencies of slightly deleterious mutations (Bengtsson 1990; Glémin 2010). Support for this model has been found in humans, where S alleles at disease causing loci tend to segregate at a higher than expected frequency (Necşulea *et al.* 2011; Lachance and Tishkoff 2014). By predicting

mutational effects with SIFT4G (Vaser *et al.* 2016), we found that gBGC is associated with selective constraint in *A. thaliana*. Genes with low average SIFT-scores, indicative of increased density of segregating harmful mutations, had a greater excess of derived S alleles (high WS/SW). The observed pattern is consistent with gBGC preventing slightly deleterious mutations from being purged by purifying selection, potentially leading to increased genetic load at genes with predominantly weak (A,T) ancestral alleles. However, our results also indicate that genes with predominantly strong (G,C) ancestral alleles may have decreased genetic load, because gBGC can facilitate the removal of new mutations, most of which are deleterious (Eyre-Walker and Keightley 2007).

Consistent with studies in mammals and birds (Galtier and Duret 2007; Galtier *et al.* 2009; Ratnakumar *et al.* 2010; Corcoran *et al.* 2017; Bolívar *et al.* 2018; Rousselle *et al.* 2019), we found evidence that gBGC influences the rate of protein evolution in *A. thaliana*, thus affecting inferences of selection that are based on patterns of nucleotide divergence and diversity. However, the increased frequency of S alleles did not lead to a false signal of positive selection, but it appears that gBGC mainly masks selection in *A. thaliana*. By comparing results from *A. thaliana* to outcrossing relatives *A. lyrata* and *C. grandiflora*, we found that measures of negative and positive selection were similarly affected in the two *Arabidopsis* species, both with small N_e , and more weakly affected in *C. grandiflora*, a species with large N_e . Although gBGC is expected to be more efficient in species with large N_e (Duret and Galtier 2009; Glémin 2010; Mugal *et al.* 2015), the association between the two parameters is not always monotonous (Galtier *et al.* 2009, 2018), particularly in protein-coding genes at which large- N_e species may be more efficient at counteracting the harmful effects of gBGC. The strength of gBGC has been decoupled from N_e in other species groups (Clément *et al.* 2017; Galtier *et al.* 2018). For instance, strong evidence of gBGC was found in the small- N_e species honey bee (Wallberg *et al.* 2015), whereas only weak evidence has been found in the large- N_e species *Drosophila melanogaster* (Galtier *et al.* 2006; Williamson *et al.* 2014). Together, these results suggest that the effects of gBGC on protein evolution cannot be simply predicted based on the mating-system and N_e . This complicates the inference of gBGC, given that estimates of the underlying parameters (gene conversion rate, track length, and repair bias) are available only for a handful of well-studied species (Galtier *et al.* 2018). In any case, we found that gBGC results in the proportion of sites fixed by positive selection to be underestimated, at least in *A. thaliana* and *A. lyrata*. For these species, the unbiased WW+SS sites could more accurately reflect the rate of adaptive evolution. This puts the α estimate for *A. thaliana* ($\alpha = 0.12$) in level with some other small- N_e species, such as humans ($\alpha = 0.14$, Uricchio *et al.* 2019), but still considerably lower than estimates for large- N_e species, such as *D. melanogaster* ($\alpha > 0.5$, Kousathanas and Keightley 2013).

Conclusions

We have shown that selective constraint is modulated by multiple genomic features in *A. thaliana*, with expression level, GC-content, and connectivity being the most influential. Importantly, our analyses provide strong evidence that gBGC shapes protein evolution in *A. thaliana*, despite the predominantly selfing mating-system. Both the increasing frequency of S alleles and the decreasing frequency of W alleles influence segregating deleterious mutations, while leading to a genome-wide signal of reduced selection-efficacy. By finding evidence that even weak outcrossing can facilitate gBGC, we have shown that it has more far-reaching consequences than previously appreciated. Based on these results, we propose that the importance of accounting for gBGC in genomic analyses should not be limited to outcrossing taxa, but it ought to be done regardless of the mating system.

Acknowledgments

We thank the associate editor, S.I. Wright, and three anonymous reviewers for their comments on improving the manuscript. Computational resources were provided by the Minnesota Supercomputing Institute (MSI) at the University of Minnesota. This work was supported by the National Science Foundation (NSF) grant IOS-1546863. Any opinions, findings, conclusions, or recommendations expressed in this material are those of the authors and do not necessarily reflect the views of the NSF.

Literature Cited

- 1001 Genomes Consortium. 2016 1,135 genomes reveal the global pattern of polymorphism in *Arabidopsis thaliana*. *Cell* 166: 481–491. <https://doi.org/10.1016/j.cell.2016.05.063>
- Agrawal, A. F., and M. C. Whitlock, 2012 Mutation load: the fitness of individuals in populations where deleterious alleles are abundant. *Annu. Rev. Ecol. Syst.* 43: 115–135. <https://doi.org/10.1146/annurev-ecolsys-110411-160257>
- Bechsgaard, J. S., V. Castric, D. Charlesworth, X. Vekemans, and M. H. Schierup, 2006 The transition to self-compatibility in *Arabidopsis thaliana* and evolution within S-Haplotypes over 10 Myr. *Mol. Biol. Evol.* 23: 1741–1750. <https://doi.org/10.1093/molbev/msl042>
- Bengtsson, B. O., 1990 The effect of biased conversion on the mutation load. *Genet. Res.* 55: 183–187. <https://doi.org/10.1017/S0016672300025519>
- Billingsley, P., 2008 *Probability and Measure*. John Wiley & Sons, Hoboken, NJ.
- Bird, A. P., 1980 DNA methylation and the frequency of CpG in animal DNA. *Nucleic Acids Res.* 8: 1499–1504. <https://doi.org/10.1093/nar/8.7.1499>
- Bolger, A. M., M. Lohse, and B. Usadel, 2014 Trimmomatic: a flexible trimmer for Illumina sequence data. *Bioinformatics* 30: 2114–2120. <https://doi.org/10.1093/bioinformatics/btu170>
- Bolívar, P., C. F. Mugal, M. Rossi, A. Nater, M. Wang *et al.*, 2018 Biased inference of selection due to GC-biased gene conversion and the rate of protein evolution in flycatchers when accounting for it. *Mol. Biol. Evol.* 35: 2475–2486. <https://doi.org/10.1093/molbev/msy149>

- Bombliès, K., L. Yant, R. A. Laitinen, S. T. Kim, J. D. Hollister *et al.*, 2010 Local-scale patterns of genetic variability, outcrossing, and spatial structure in natural stands of *Arabidopsis thaliana*. *PLoS Genet.* 6: e1000890. <https://doi.org/10.1371/journal.pgen.1000890>
- Breiman, L., 2001 Random forests. *Mach. Learn.* 45: 5–32. <https://doi.org/10.1023/A:1010933404324>
- Browning, B. L., Y. Zhou, and S. R. Browning, 2018 A one-penny imputed genome from next-generation reference panels. *Am. J. Hum. Genet.* 103: 338–348. <https://doi.org/10.1016/j.ajhg.2018.07.015>
- Bustamante, C. D., R. Nielsen, S. A. Sawyer, K. M. Olsen, M. D. Purugganan *et al.*, 2002 The cost of inbreeding in *Arabidopsis*. *Nature* 416: 531–534. <https://doi.org/10.1038/416531a>
- Camacho, C., G. Coulouris, V. Avagyan, N. Ma, J. Papadopoulos *et al.*, 2009 BLAST+: architecture and applications. *BMC Bioinformatics* 10: 421. <https://doi.org/10.1186/1471-2105-10-421>
- Cao, J., K. Schneeberger, S. Ossowski, T. Günther, S. Bender *et al.*, 2011 Whole-genome sequencing of multiple *Arabidopsis thaliana* populations. *Nat. Genet.* 43: 956–963. <https://doi.org/10.1038/ng.911>
- Charif, D., and J. R. Lobry, 2007 SeqinR 1.0–2: a contributed package to the R project for statistical computing devoted to biological sequences retrieval and analysis, pp. 207–232 in *Structural Approaches to Sequence Evolution*. Springer, Berlin, Heidelberg.
- Charlesworth, B., and D. Charlesworth, 1998 Some evolutionary consequences of deleterious mutations. *Genetica* 102–103: 3–19. <https://doi.org/10.1023/A:1017066304739>
- Charlesworth, D., M. T. Morgan, and B. Charlesworth, 1993 Mutation accumulation in finite outbreeding and inbreeding populations. *Genet. Res.* 61: 39–56. <https://doi.org/10.1017/S0016672300031086>
- Charlesworth, J., and A. Eyre-Walker, 2008 The McDonald-Kreitman test and slightly deleterious mutations. *Mol. Biol. Evol.* 25: 1007–1015. <https://doi.org/10.1093/molbev/msn005>
- Chen, J., S. Glémin, and M. Lascoux, 2017 Genetic diversity and the efficacy of purifying selection across plant and animal species. *Mol. Biol. Evol.* 34: 1417–1428. <https://doi.org/10.1093/molbev/msx088>
- Chun, S., and J. C. Fay, 2011 Evidence for hitchhiking of deleterious mutations within the human genome. *PLoS Genet.* 7: e1002240. <https://doi.org/10.1371/journal.pgen.1002240>
- Clément, Y., G. Sarah, Y. Holtz, F. Homa, S. Pointet *et al.*, 2017 Evolutionary forces affecting synonymous variations in plant genomes. *PLoS Genet.* 13: e1006799. <https://doi.org/10.1371/journal.pgen.1006799>
- Corcoran, P., T. I. Gossmann, H. J. Barton, J. Slate, K. Zeng *et al.*, 2017 Determinants of the efficacy of natural selection on coding and noncoding variability in two passerine species. *Genome Biol. Evol.* 9: 2987–3007. <https://doi.org/10.1093/gbe/evx213>
- Crow, J. F., 1970 Genetic loads and the cost of natural selection, pp. 128–177 in *Mathematical Topics in Population Genetics*. Springer, Berlin, Heidelberg. https://doi.org/10.1007/978-3-642-46244-3_5
- Cutter, A. D., and B. A. Payseur, 2013 Genomic signatures of selection at linked sites: unifying the disparity among species. *Nat. Rev. Genet.* 14: 262–274. <https://doi.org/10.1038/nrg3425>
- Danecek, P., A. Auton, G. Abecasis, C. A. Albers, E. Banks *et al.*, 2011 The variant call format and VCFtools. *Bioinformatics* 27: 2156–2158. <https://doi.org/10.1093/bioinformatics/btr330>
- Douglas, G. M., G. Gos, K. A. Steige, A. Salcedo, K. Holm *et al.*, 2015 Hybrid origins and the earliest stages of diploidization in the highly successful recent polyploid *Capsella bursa-pastoris*. *Proc. Natl. Acad. Sci. USA* 112: 2806–2811. <https://doi.org/10.1073/pnas.1412277112>
- Duret, L., and N. Galtier, 2009 Biased gene conversion and the evolution of mammalian genomic landscapes. *Annu. Rev. Genomics Hum. Genet.* 10: 285–311. <https://doi.org/10.1146/annurev-genom-082908-150001>
- Durvasula, A., A. Fulgione, R. M. Gutaker, S. I. Alacakaptan, P. J. Flood *et al.*, 2017 African genomes illuminate the early history and transition to selfing in *Arabidopsis thaliana*. *Proc. Natl. Acad. Sci. USA* 114: 5213–5218. <https://doi.org/10.1073/pnas.1616736114>
- Eyre-Walker, A., 1993 Recombination and mammalian genome evolution. *Proc. Biol. Sci.* 252: 237–243.
- Eyre-Walker, A., and P. D. Keightley, 2007 The distribution of fitness effects of new mutations. *Nat. Rev. Genet.* 8: 610–618. <https://doi.org/10.1038/nrg2146>
- Eyre-Walker, A., and P. D. Keightley, 2009 Estimating the rate of adaptive molecular evolution in the presence of slightly deleterious mutations and population size change. *Mol. Biol. Evol.* 26: 2097–2108. <https://doi.org/10.1093/molbev/msp119>
- Fay, J. C., 2011 Weighing the evidence for adaptation at the molecular level. *Trends Genet.* 27: 343–349. <https://doi.org/10.1016/j.tig.2011.06.003>
- Felsenstein, J., 1974 The evolutionary advantage of recombination. *Genetics* 78: 737–756.
- Fraser, H. B., A. E. Hirsh, L. M. Steinmetz, C. Scharfe, and M. W. Feldman, 2002 Evolutionary rate in the protein interaction network. *Science* 296: 750–752. <https://doi.org/10.1126/science.1068696>
- Galtier, N., and L. Duret, 2007 Adaptation or biased gene conversion? Extending the null hypothesis of molecular evolution. *Trends Genet.* 23: 273–277. <https://doi.org/10.1016/j.tig.2007.03.011>
- Galtier, N., G. Piganeau, D. Mounchiroud, and L. Duret, 2001 GC-content evolution in mammalian genomes: the biased gene conversion hypothesis. *Genetics* 159: 907–911.
- Galtier, N., E. Bazin, and N. Bierne, 2006 GC-biased segregation of noncoding polymorphisms in *Drosophila*. *Genetics* 172: 221–228. <https://doi.org/10.1534/genetics.105.046524>
- Galtier, N., L. Duret, S. Glémin, and V. Ranwez, 2009 GC-biased gene conversion promotes the fixation of deleterious amino acid changes in primates. *Trends Genet.* 25: 1–5. <https://doi.org/10.1016/j.tig.2008.10.011>
- Galtier, N., C. Roux, M. Rousselle, J. Romiguier, E. Figuet *et al.*, 2018 Codon usage bias in animals: disentangling the effects of natural selection, effective population size, and GC-biased gene conversion. *Mol. Biol. Evol.* 35: 1092–1103. <https://doi.org/10.1093/molbev/msy015>
- Geurts, P., D. Ernst, and L. Wehenkel, 2006 Extremely randomized trees. *Mach. Learn.* 63: 3–42. <https://doi.org/10.1007/s10994-006-6226-1>
- Giraut, L., M. Falque, J. Drouaud, L. Pereira, O. C. Martin *et al.*, 2011 Genome-wide crossover distribution in *Arabidopsis thaliana* meiosis reveals sex-specific patterns along chromosomes. *PLoS Genet.* 7: e1002354. <https://doi.org/10.1371/journal.pgen.1002354>
- Glémin, S., 2010 Surprising fitness consequences of GC-biased gene conversion: I. Mutation load and inbreeding depression. *Genetics* 185: 939–959 [corrigenda: *Genetics* 190: 1585 (2012)]. <https://doi.org/10.1534/genetics.110.116368>
- Glémin, S., Y. Clément, J. David, and A. Ressayre, 2014 GC content evolution in coding regions of angiosperm genomes: a unifying hypothesis. *Trends Genet.* 30: 263–270. <https://doi.org/10.1016/j.tig.2014.05.002>
- Glémin, S., P. F. Arndt, P. W. Messer, D. Petrov, N. Galtier *et al.*, 2015 Quantification of GC-biased gene conversion in the human genome. *Genome Res.* 25: 1215–1228. <https://doi.org/10.1101/gr.185488.114>
- Gossmann, T. I., B. H. Song, A. J. Windsor, T. Mitchell-Olds, C. J. Dixon *et al.*, 2010 Genome wide analyses reveal little evidence for adaptive evolution in many plant species. *Mol. Biol. Evol.* 27: 1822–1832. <https://doi.org/10.1093/molbev/msq079>

- Gossmann, T. I., P. D. Keightley, and A. Eyre-Walker, 2012 The effect of variation in the effective population size on the rate of adaptive molecular evolution in eukaryotes. *Genome Biol. Evol.* 4: 658–667. <https://doi.org/10.1093/gbe/evs027>
- Günther, T., C. Lampe, and K. J. Schmid, 2013 Mutational bias and gene conversion affect the intraspecific nitrogen stoichiometry of the *Arabidopsis thaliana* transcriptome. *Mol. Biol. Evol.* 30: 561–568. <https://doi.org/10.1093/molbev/mss249>
- Haldane, J. B. S., 1937 The effect of variation on fitness. *Am. Nat.* 71: 337–349. <https://doi.org/10.1086/280722>
- Haller, B. C., and P. W. Messer, 2019 SLiM 3: forward genetic simulations beyond the Wright–Fisher model. *Mol. Biol. Evol.* 36: 632–637. <https://doi.org/10.1093/molbev/msy228>
- Hämälä, T., and O. Savolainen, 2019 Genomic patterns of local adaptation under gene flow in *Arabidopsis lyrata*. *Mol. Biol. Evol.* 36: 2557–2571. <https://doi.org/10.1093/molbev/msz149>
- Hämälä, T., T. M. Mattila, P. H. Leinonen, H. Kuittinen, and O. Savolainen, 2017 Role of seed germination in adaptation and reproductive isolation in *Arabidopsis lyrata*. *Mol. Ecol.* 26: 3484–3496. <https://doi.org/10.1111/mec.14135>
- Hämälä, T., T. M. Mattila, and O. Savolainen, 2018 Local adaptation and ecological differentiation under selection, migration and drift in *Arabidopsis lyrata*. *Evolution*. 72: 1373–1386. <https://doi.org/10.1111/evo.13502>
- Hämälä, T., M. J. Guiltinan, J. H. Marden, S. N. Maximova, C. W. DePamphilis *et al.*, 2020 Gene expression modularity reveals footprints of polygenic adaptation in *Theobroma cacao*. *Mol. Biol. Evol.* 37: 110–123. <https://doi.org/10.1093/molbev/msz206>
- Hartfield, M., and S. P. Otto, 2011 Recombination and hitchhiking of deleterious alleles. *Evolution*. 65: 2421–2434. <https://doi.org/10.1111/j.1558-5646.2011.01311.x>
- Hazzouri, K. M., J. S. Escobar, R. W. Ness, L. Killian Newman, A. M. Randle *et al.*, 2013 Comparative population genomics in *Collinsia* sister species reveals evidence for reduced effective population size, relaxed selection, and evolution of biased gene conversion with an ongoing mating system shift. *Evolution*. 67: 1263–1278.
- Hill, W. G., and A. Robertson, 1966 The effects of linkage and the limits to artificial selection. *Genet. Res.* 8: 269–294. <https://doi.org/10.1017/S0016672300010156>
- Hu, T. T., P. Pattyn, E. G. Bakker, J. Cao, J.-F. Cheng *et al.*, 2011 The *Arabidopsis lyrata* genome sequence and the basis of rapid genome size change. *Nat. Genet.* 43: 476–481. <https://doi.org/10.1038/ng.807>
- Josephs, E. B., S. I. Wright, J. R. Stinchcombe, and D. J. Schoen, 2017 The relationship between selection, network connectivity, and regulatory variation within a population of *Capsella grandiflora*. *Genome Biol. Evol.* 9: 1099–1109. <https://doi.org/10.1093/gbe/evx068>
- Jukes, T. H., and C. R. Cantor, 1969 Evolution of protein molecules. *Mamm. Protein Metab.* 3: 21–132. <https://doi.org/10.1016/B978-1-4832-3211-9.50009-7>
- Kawakatsu, T., S.-S. Carol Huang, F. Jupe, E. Sasaki, R. J. Schmitz *et al.*, 2016 Epigenomic diversity in a global collection of *Arabidopsis thaliana* accessions. *Cell* 166: 492–505. <https://doi.org/10.1016/j.cell.2016.06.044>
- Keightley, P. D., and S. P. Otto, 2006 Interference among deleterious mutations favours sex and recombination in finite populations. *Nature* 443: 89–92. <https://doi.org/10.1038/nature05049>
- Keightley, P. D., and A. Eyre-Walker, 2007 Joint inference of the distribution of fitness effects of deleterious mutations and population demography based on nucleotide polymorphism frequencies. *Genetics* 177: 2251–2261. <https://doi.org/10.1534/genetics.107.080663>
- Keightley, P. D., and B. C. Jackson, 2018 Inferring the probability of the derived vs. the ancestral allelic state at a polymorphic site. *Genetics* 209: 897–906.
- Kim, S., 2015 ppcor: an R package for a fast calculation to semi-partial correlation coefficients. *Commun. Stat. Appl. Methods* 22: 665.
- Kim, Y., and T. Wiehe, 2008 Simulation of DNA sequence evolution under models of recent directional selection. *Brief. Bioinform.* 10: 84–96. <https://doi.org/10.1093/bib/bbn048>
- Klemm, S. L., Z. Shipony, and W. J. Greenleaf, 2019 Chromatin accessibility and the regulatory epigenome. *Nat. Rev. Genet.* 20: 207–220. <https://doi.org/10.1038/s41576-018-0089-8>
- Koenig, D., J. Hagmann, R. Li, F. Bemm, T. Slotte *et al.*, 2019 Long-term balancing selection drives evolution of immunity genes in *Capsella*. *eLife* 8: e43606. <https://doi.org/10.7554/eLife.43606>
- Kono, T. J. Y., L. Lei, C. H. Shih, P. J. Hoffman, P. L. Morrell *et al.*, 2018 Comparative genomics approaches accurately predict deleterious variants in plants. *G3 Genes, Genomes. Genet.* 8: 3321–3329.
- Koonin, E. V., 2011 Are there laws of genome evolution? *PLoS Comput. Biol.* 7: e1002173. <https://doi.org/10.1371/journal.pcbi.1002173>
- Kousathanas, A., and P. D. Keightley, 2013 A comparison of models to infer the distribution of fitness effects of new mutations. *Genetics* 193: 1197–1208. <https://doi.org/10.1534/genetics.112.148023>
- Kuhn, M., 2008 Building predictive models in R using the caret package. *J. Stat. Softw.* 28: 1–26. <https://doi.org/10.18637/jss.v028.i05>
- Lachance, J., and S. A. Tishkoff, 2014 Biased gene conversion skews allele frequencies in human populations, increasing the disease burden of recessive alleles. *Am. J. Hum. Genet.* 95: 408–420. <https://doi.org/10.1016/j.ajhg.2014.09.008>
- Lamesch, P., T. Z. Berardini, D. Li, D. Swarbreck, C. Wilks *et al.*, 2012 The Arabidopsis Information Resource (TAIR): improved gene annotation and new tools. *Nucleic Acids Res.* 40: D1202–D1210. <https://doi.org/10.1093/nar/gkr1090>
- Langfelder, P., and S. Horvath, 2008 WGCNA: an R package for weighted correlation network analysis. *BMC Bioinformatics* 9: 559. <https://doi.org/10.1186/1471-2105-9-559>
- Leseqque, Y., D. Mouchiroud, and L. Duret, 2013 GC-biased gene conversion in yeast is specifically associated with crossovers: molecular mechanisms and evolutionary significance. *Mol. Biol. Evol.* 30: 1409–1419. <https://doi.org/10.1093/molbev/mst056>
- Li, H., 2011 A statistical framework for SNP calling, mutation discovery, association mapping and population genetical parameter estimation from sequencing data. *Bioinformatics* 27: 2987–2993. <https://doi.org/10.1093/bioinformatics/btr509>
- Li, H., 2013 Aligning sequence reads, clone sequences and assembly contigs with BWA-MEM. *arXiv:1303.3997v2* [q-bio.GN].
- Li, H., B. Handsaker, A. Wysoker, T. Fennell, J. Ruan *et al.*, 2009 The sequence alignment/map format and SAMtools. *Bioinformatics* 25: 2078–2079. <https://doi.org/10.1093/bioinformatics/btp352>
- Liu, H., J. Huang, X. Sun, J. Li, Y. Hu *et al.*, 2018 Tetrad analysis in plants and fungi finds large differences in gene conversion rates but no GC bias. *Nat. Ecol. Evol.* 2: 164–173. <https://doi.org/10.1038/s41559-017-0372-7>
- Lloyd, A., C. Morgan, F. C. H. Franklin, and K. Bomblies, 2018 Plasticity of meiotic recombination rates in response to temperature in *Arabidopsis*. *Genetics* 208: 1409–1420. <https://doi.org/10.1534/genetics.117.300588>
- Löytynoja, A., and N. Goldman, 2008 Phylogeny-aware gap placement prevents errors in sequence alignment and evolutionary analysis. *Science* 320: 1632–1635. <https://doi.org/10.1126/science.1158395>
- Lu, Z., A. P. Marand, W. A. Ricci, C. L. Ethridge, X. Zhang *et al.*, 2019 The prevalence, evolution and chromatin signatures of plant regulatory elements. *Nat. Plants* 5: 1250–1259. <https://doi.org/10.1038/s41477-019-0548-z>

- Lynch, M., and W. Gabriel, 1990 Mutation load and the survival of small populations. *Evolution* 44: 1725–1737. <https://doi.org/10.1111/j.1558-5646.1990.tb05244.x>
- Mancera, E., R. Bourgon, A. Brozzi, W. Huber, and L. M. Steinmetz, 2008 High-resolution mapping of meiotic crossovers and non-crossovers in yeast. *Nature* 454: 479–485. <https://doi.org/10.1038/nature07135>
- Marais, G., 2003 Biased gene conversion: implications for genome and sex evolution. *Trends Genet.* 19: 330–338. [https://doi.org/10.1016/S0168-9525\(03\)00116-1](https://doi.org/10.1016/S0168-9525(03)00116-1)
- Marais, G., B. Charlesworth, and S. I. Wright, 2004 Recombination and base composition: the case of the highly self-fertilizing plant *Arabidopsis thaliana*. *Genome Biol.* 5: R45.
- Marçais, G., A. L. Delcher, A. M. Phillippy, R. Coston, S. L. Salzberg *et al.*, 2018 MUMmer4: a fast and versatile genome alignment system. *PLoS Comput. Biol.* 14: e1005944. <https://doi.org/10.1371/journal.pcbi.1005944>
- Mattila, T. M., J. Tyrmä, T. Pyhäjärvi, and O. Savolainen, 2017 Genome-wide analysis of colonization history and concomitant selection in *Arabidopsis lyrata*. *Mol. Biol. Evol.* 34: 2665–2677. <https://doi.org/10.1093/molbev/msx193>
- Mattila, T. M., B. Laenen, R. Horvath, T. Hämälä, O. Savolainen *et al.*, 2019 Impact of demography on linked selection in two outcrossing Brassicaceae species. *Ecol. Evol.* 9: 9532–9545. <https://doi.org/10.1002/ece3.5463>
- McDonald, J. H., and M. Kreitman, 1991 Adaptive protein evolution at the *Adh* locus in *Drosophila*. *Nature* 351: 652–654. <https://doi.org/10.1038/351652a0>
- Mugal, C. F., C. C. Weber, and H. Ellegren, 2015 GC-biased gene conversion links the recombination landscape and demography to genomic base composition: GC-biased gene conversion drives genomic base composition across a wide range of species. *BioEssays* 37: 1317–1326. <https://doi.org/10.1002/bies.201500058>
- Muller, H., 1950 Our load of mutations. *Am. J. Hum. Genet.* 2: 111–176.
- Muller, H., 1964 The relation of recombination to mutational advance. *Mutat. Res.* 1: 2–9. [https://doi.org/10.1016/0027-5107\(64\)90047-8](https://doi.org/10.1016/0027-5107(64)90047-8)
- Muyle, A., L. Serres-Gardi, A. Ressayre, J. Escobar, and S. Glémin, 2011 GC-biased gene conversion and selection affect GC content in the *Oryza* genus (rice). *Mol. Biol. Evol.* 28: 2695–2706. <https://doi.org/10.1093/molbev/msr104>
- Necşulea, A., A. Popa, D. N. Cooper, P. D. Stenson, D. Mouchiroud *et al.*, 2011 Meiotic recombination favors the spreading of deleterious mutations in human populations. *Hum. Mutat.* 32: 198–206. <https://doi.org/10.1002/humu.21407>
- Nembrini, S., I. R. König, and M. N. Wright, 2018 The revival of the Gini importance? *Bioinformatics* 34: 3711–3718. <https://doi.org/10.1093/bioinformatics/bty373>
- Nielsen, R., 2005 Molecular signatures of natural selection. *Annu. Rev. Genet.* 39: 197–218. <https://doi.org/10.1146/annurev.genet.39.073003.112420>
- Nordborg, M., 2000 Linkage disequilibrium, gene trees and selfing: an ancestral recombination graph with partial self-fertilization. *Genetics* 154: 923–929.
- Novembre, J. A., 2002 Accounting for background nucleotide composition when measuring codon usage bias. *Mol. Biol. Evol.* 19: 1390–1394. <https://doi.org/10.1093/oxfordjournals.molbev.a004201>
- Ohta, T., 1973 Slightly deleterious mutant substitutions in evolution. *Nature* 246: 96–98. <https://doi.org/10.1038/246096a0>
- Papakostas, S., L. A. Vøllestad, M. Bruneaux, T. Aykanat, J. Vanoverbeke *et al.*, 2014 Gene pleiotropy constrains gene expression changes in fish adapted to different thermal conditions. *Nat. Commun.* 5: 4071. <https://doi.org/10.1038/ncomms5071>
- Peck, J. R., 1994 A ruby in the rubbish: beneficial mutations, deleterious mutations and the evolution of sex. *Genetics* 137: 597–606.
- Pessia, E., A. Popa, S. Mousset, C. Rezvoy, L. Duret *et al.*, 2012 Evidence for widespread GC-biased gene conversion in eukaryotes. *Genome Biol. Evol.* 4: 675–682. <https://doi.org/10.1093/gbe/evs052>
- Pollak, E., 1987 On the theory of partially inbreeding finite populations. I. Partial selfing. *Genetics* 117: 353–360.
- Ratnakumar, A., S. Mousset, S. Glémin, J. Berglund, N. Galtier *et al.*, 2010 Detecting positive selection within genomes: the problem of biased gene conversion. *Philos. Trans. R. Soc. B Biol. Sci.* 365: 2571–2580.
- Rauscher, M. D., R. E. Miller, and P. Tiffin, 1999 Patterns of evolutionary rate variation among genes of the anthocyanin biosynthetic pathway. *Mol. Biol. Evol.* 16: 266–274. <https://doi.org/10.1093/oxfordjournals.molbev.a026108>
- Rodgers-Melnick, E., D. Vera, H. Bass, and E. Buckler, 2016 Open chromatin reveals the functional maize genome. *Proc. Natl. Acad. Sci. USA* 113: E3177–E3184. <https://doi.org/10.1073/pnas.1525244113>
- Ross-Ibarra, J., P. L. Morrell, and B. S. Gaut, 2007 Plant domestication, a unique opportunity to identify the genetic basis of adaptation. *Proc. Natl. Acad. Sci. USA* 104: 8641–8648. <https://doi.org/10.1073/pnas.0700643104>
- Rousselle, M., A. Laverré, E. Figuet, B. Nabholz, and N. Galtier, 2019 Influence of recombination and GC-biased gene conversion on the adaptive and nonadaptive substitution rate in mammals vs. birds. *Mol. Biol. Evol.* 36: 458–471. <https://doi.org/10.1093/molbev/msy243>
- Rowan, B. A., D. Heavens, T. R. Feuerborn, A. J. Tock, I. R. Henderson *et al.*, 2019 An ultra high-density *Arabidopsis thaliana* crossover map that refines the influence of structural variation and epigenetic features. *Genetics* 213: 771–787. <https://doi.org/10.1534/genetics.119.302406>
- Sellinger, T. P. P., D. A. Awad, M. Moest, and A. Tellier, 2020 Inference of past demography, dormancy and self-fertilization rates from whole genome sequence data. *PLoS Genet.* 16: e1008698. <https://doi.org/10.1371/journal.pgen.1008698>
- Slotte, T., J. P. Foxe, K. M. Hazzouri, and S. I. Wright, 2010 Genome-wide evidence for efficient positive and purifying selection in *Capsella grandiflora*, a plant species with a large effective population size. *Mol. Biol. Evol.* 27: 1813–1821. <https://doi.org/10.1093/molbev/msq062>
- Slotte, T., T. Bataillon, T. T. Hansen, K. St. Onge, S. I. Wright *et al.*, 2011 Genomic determinants of protein evolution and polymorphism in *Arabidopsis*. *Genome Biol. Evol.* 3: 1210–1219. <https://doi.org/10.1093/gbe/evr094>
- Slotte, T., K. M. Hazzouri, D. Stern, P. Andolfatto, and S. I. Wright, 2012 Genetic architecture and adaptive significance of the selfing syndrome in *Capsella*. *Evolution*. 66: 1360–1374. <https://doi.org/10.1111/j.1558-5646.2011.01540.x>
- Slotte, T., K. M. Hazzouri, J. A. Ågren, D. Koenig, F. Maumus *et al.*, 2013 The *Capsella rubella* genome and the genomic consequences of rapid mating system evolution. *Nat. Genet.* 45: 831–835. <https://doi.org/10.1038/ng.2669>
- Smeds, L., C. F. Mugal, A. Qvarnström, and H. Ellegren, 2016 High-resolution mapping of crossover and non-crossover recombination events by whole-genome re-sequencing of an avian pedigree. *PLoS Genet.* 12: e1006044. <https://doi.org/10.1371/journal.pgen.1006044>
- Stapley, J., P. G. D. Feulner, S. E. Johnston, A. W. Santure, and C. M. Smadja, 2017 Variation in recombination frequency and distribution across eukaryotes: Patterns and processes. *Philos. Trans. R. Soc. Lond. B Biol. Sci.* 372: 20160455 (erratum: *Philos. Trans. R. Soc. Lond. B Biol. Sci.* 373: 2017.0360).
- Steige, K. A., B. Laenen, J. Reimegård, D. G. Scofield, and T. Slotte, 2017 Genomic analysis reveals major determinants of cis-regulatory variation in *Capsella grandiflora*. *Proc. Natl. Acad. Sci. USA* 114: 1087–1092. <https://doi.org/10.1073/pnas.1612561114>
- Tajima, F., 1983 Evolutionary relationship of DNA sequences in finite populations. *Genetics* 105: 437–460.

- Tajima, F., 1989 Statistical method for testing the neutral mutation hypothesis by DNA polymorphism. *Genetics* 123: 585–595.
- Tang, C., C. Toomajian, S. Sherman-Broyles, V. Plagnol, Y. L. Guo *et al.*, 2007 The evolution of selfing in *Arabidopsis thaliana*. *Science* 317: 1070–1072. <https://doi.org/10.1126/science.1143153>
- Uricchio, L. H., D. A. Petrov, and D. Enard, 2019 Exploiting selection at linked sites to infer the rate and strength of adaptation. *Nat. Ecol. Evol.* 3: 977–984. <https://doi.org/10.1038/s41559-019-0890-6>
- Vaser, R., A. Adusumalli, S. N. Leng, M. Sikic, and P. C. Ng, 2016 SIFT missense predictions for genomes. *Nat. Protoc.* 11: 1–9. <https://doi.org/10.1038/nprot.2015.123>
- Wallberg, A., S. Glémin, and M. T. Webster, 2015 Extreme recombination frequencies shape genome variation and evolution in the honeybee, *Apis mellifera*. *PLoS Genet.* 11: e1005189. <https://doi.org/10.1371/journal.pgen.1005189>
- Weng, M. L., C. Becker, J. Hildebrandt, M. Neumann, M. T. Rutter *et al.*, 2019 Fine-grained analysis of spontaneous mutation spectrum and frequency in *Arabidopsis thaliana*. *Genetics* 211: 703–714. <https://doi.org/10.1534/genetics.118.301721>
- Wijnker, E., G. V. James, J. Ding, F. Becker, J. R. Klasen *et al.*, 2013 The genomic landscape of meiotic crossovers and gene conversions in *Arabidopsis thaliana*. *eLife* 2013: 1–22.
- Williamson, R. J., E. B. Josephs, A. E. Platts, K. M. Hazzouri, A. Haudry *et al.*, 2014 Evidence for widespread positive and negative selection in coding and conserved noncoding regions of *capsella grandiflora*. *PLoS Genet.* 10: e1004622. <https://doi.org/10.1371/journal.pgen.1004622>
- Willing, E. M., V. Rawat, T. Mandáková, F. Maumus, G. V. James *et al.*, 2015 Genome expansion of *Arabidopsis alpina* linked with retrotransposition and reduced symmetric DNA methylation. *Nat. Plants* 1: 14023. <https://doi.org/10.1038/nplants.2014.23>
- Wright, M. N., and A. Ziegler, 2017 ranger: a fast implementation of random forests for high dimensional data in C++ and R. *J. Stat. Softw.* 77: 1–17. <https://doi.org/10.18637/jss.v077.i01>
- Yang, S., Y. Yuan, L. Wang, J. Li, W. Wang *et al.*, 2012 Great majority of recombination events in *Arabidopsis* are gene conversion events. *Proc. Natl. Acad. Sci. USA* 109: 20992–20997. <https://doi.org/10.1073/pnas.1211827110>
- Zhang, M., L. Zhou, R. Bawa, H. Suren, and J. A. Holliday, 2016 Recombination rate variation, hitchhiking, and demographic history shape deleterious load in poplar. *Mol. Biol. Evol.* 33: 2899–2910. <https://doi.org/10.1093/molbev/msw169>

Communicating editor: S. Wright